Crystal structure of valbenazine, $C_{24}H_{38}N_2O_4$

Tawnee M. Ens,[1] James A. Kaduk,[2,3,a)] Megan M. Rost,[4] Anja Dosen,[4] and Thomas N. Blanton[4]
[1]*North Central College, 131 S. Loomis St., Naperville, IL 60540, USA*
[2]*Illinois Institute of Technology, 3101 S. Dearborn St., Chicago, IL 60616, USA*
[3]*North Central College, 131 S. Loomis St., Naperville, IL 60540, USA*
[4]*ICDD, 12 Campus Blvd., Newtown Square, PA 19073-3273, USA*

(Received 26 January 2024; accepted 26 March 2024)

The crystal structure of valbenazine has been solved and refined using synchrotron X-ray powder diffraction data and optimized using density functional theory techniques. Valbenazine crystallizes in space group $P2_12_12_1$ (#19) with $a = 5.260267(17)$, $b = 17.77028(7)$, $c = 26.16427(9)$ Å, $V = 2445.742(11)$ Å^3, and $Z = 4$ at 295 K. The crystal structure consists of discrete molecules and the mean plane of the molecules is approximately (8,−2,15). There are no obvious strong intermolecular interactions. There is only one weak classical hydrogen bond in the structure, from the amino group to the ether oxygen atom. Two intramolecular and one intermolecular C–H···O hydrogen bonds also contribute to the lattice energy. The powder pattern has been submitted to ICDD for inclusion in the Powder Diffraction File™ (PDF®)

[doi:10.1017/S0885715624000198]

Keywords: valbenazine, Ingrezza®, crystal structure, Rietveld refinement, density functional theory

I. INTRODUCTION

Valbenazine (marketed under the trade name Ingrezza®) is used to treat tardive dyskinesia, a disorder that results in involuntary repetitive body movements. The systematic name (CAS Registry Number 1025504-45-3) is [(2R,3R,11bR)-9,10-dimethoxy-3-(2-methylpropyl)-2,3,4,6,7,11b-hexahydro-1H-benzo[a]quinolizin-2-yl] (2S)-2-amino-3-methylbutanoate. A two-dimensional molecular diagram of valbenazine is shown in Figure 1.

X-ray powder diffraction patterns of several polymorphs of valbenazine ditosylate and dihydrochloride are reported in International Patent Application WO 2017/075340 A1 (McGee et al., 2017; Neurocrine Biosciences) and the equivalent US application US 2017/0145008 A1. A powder pattern for valbenazine free base is reported in WO 2018/130345 A1 (Langes and Reissmann, 2018; Sandoz); however, no crystal structure was reported.

This work was carried out as part of a project (Kaduk et al., 2014) to determine the crystal structures of large-volume commercial pharmaceuticals and include high-quality powder diffraction data for them in the Powder Diffraction File (Gates-Rector and Blanton, 2019).

II. EXPERIMENTAL

Valbenazine was a commercial reagent, purchased from AchemBlock (Batch #8384), and was used as-received. The yellowish white powder was packed into a 1.5 mm diameter Kapton capillary and rotated during the measurement at ~50 Hz. The powder pattern was measured at 295 K at beam line 11-BM (Antao et al., 2008; Lee et al., 2008; Wang et al., 2008) of the Advanced Photon Source at Argonne National Laboratory using a wavelength of 0.459744(2) Å from 0.5 to 40° 2θ with a step size of 0.001° and a counting time of 0.1 s/step. The high-resolution powder diffraction data were collected using 12 silicon crystal

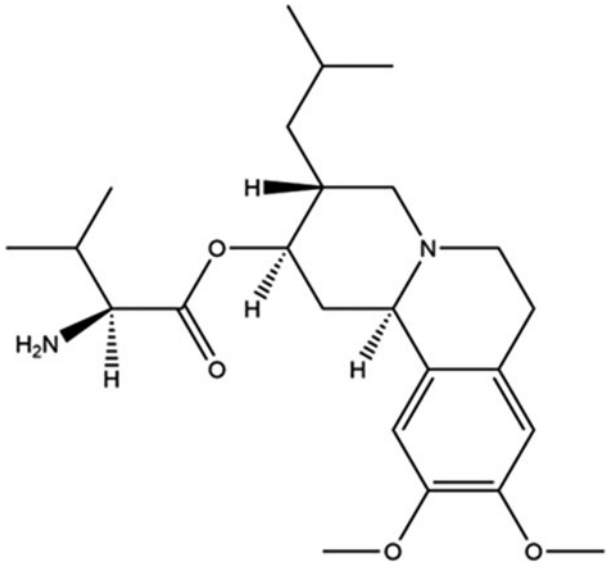

Figure 1. The two-dimensional structure of valbenazine.

a)Author to whom correspondence should be addressed. Electronic mail: kaduk@polycrystallography.com

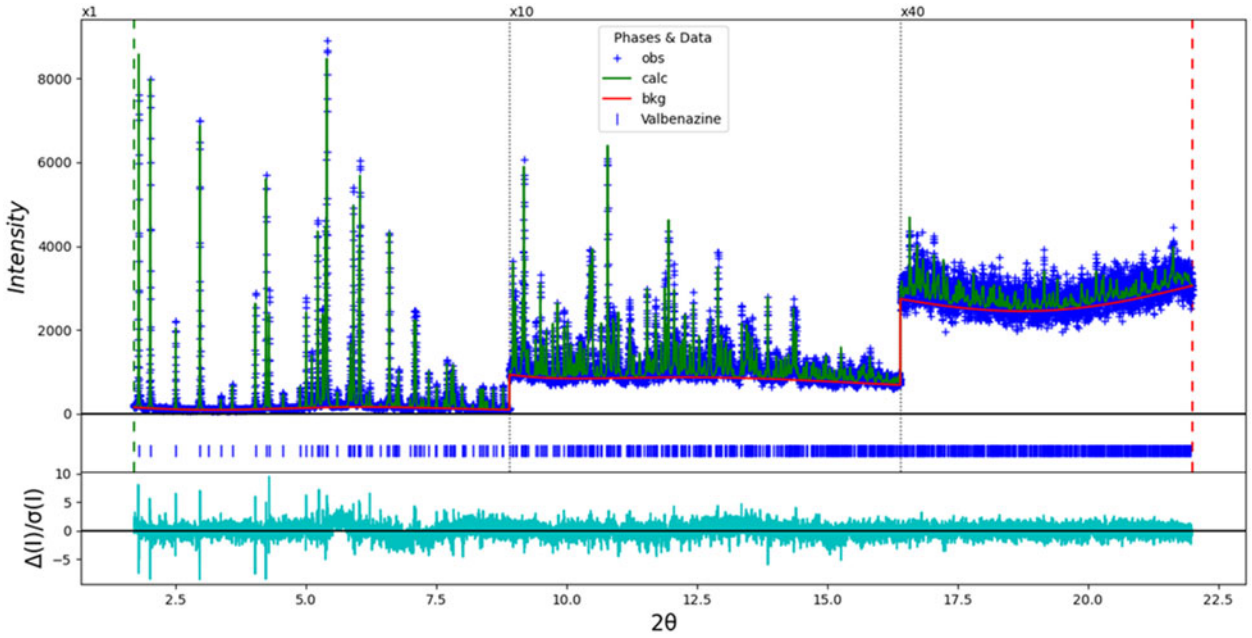

Figure 2. The Rietveld plot for the refinement of valbenazine. The blue crosses represent the observed data points, and the green line is the calculated pattern. The cyan curve is the normalized error plot, and the red line is the background curve. The vertical scale (counts) has been multiplied by a factor of 10× for $2\theta > 9.5°$, and 40× for $2\theta > 16.5°$.

analyzers that allow for high angular resolution, high precision, and accurate peak positions. A mixture of silicon (NIST SRM 640c) and alumina (NIST SRM 676a) standards (ratio Al_2O_3:Si = 2:1 by weight) was used to calibrate the instrument and refine the monochromatic wavelength used in the experiment.

The pattern was indexed using N-TREOR (Altomare et al., 2013) on a primitive orthorhombic unit cell with $a =$ 5.26085, $b = 17.77338$, $c = 26.16453$ Å, $V = 2446.5$ Å^3, and $Z = 4$. The suggested space group was $P2_12_12_1$, which was confirmed by the successful solution and refinement of the structure. A reduced cell search of the Cambridge Structural Database (Groom et al., 2016) yielded 19 hits, but no structures of valbenazine or its derivatives.

The valbenazine molecule was downloaded from PubChem (Kim et al., 2023) as Conformer3D_CID_24795069.sdf. It was converted to a *.mol2 file using Mercury (Macrae et al., 2020), and to a Fenske–Hall *Z*-matrix using OpenBabel (O'Boyle et al., 2011). The crystal structure was solved using Monte Carlo simulated annealing techniques as implemented in FOX (Favre-Nicolin and Černý, 2002), using $(\sin\theta/\lambda)_{max} = 0.3$ Å^{-1}.

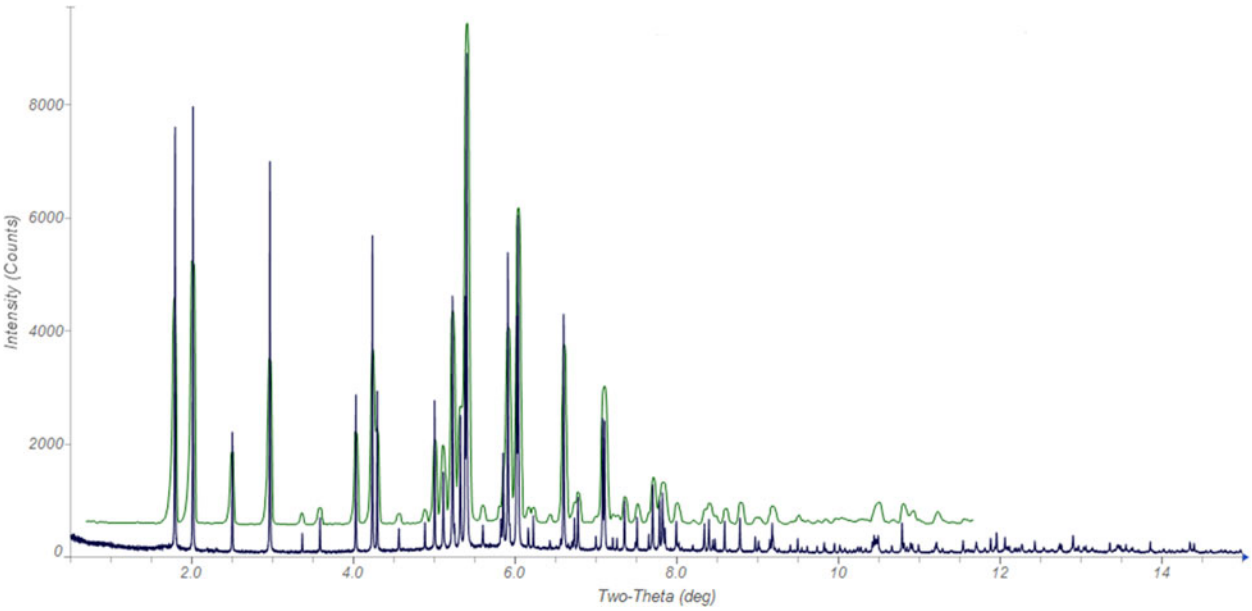

Figure 3. Comparison of the synchrotron pattern of valbenazine (black) from this study to that reported by Langes and Reissmann (2018; green). The literature pattern (measured using Cu K_α radiation) was digitized using UN-SCAN-IT (Silk Scientific, 2013) and converted to the synchrotron wavelength of 0.459744(2) Å using JADE Pro (MDI, 2023). Image generated using JADE Pro (MDI, 2023).

https://doi.org/10.1017/S0885715624000198 Published online by Cambridge University Press

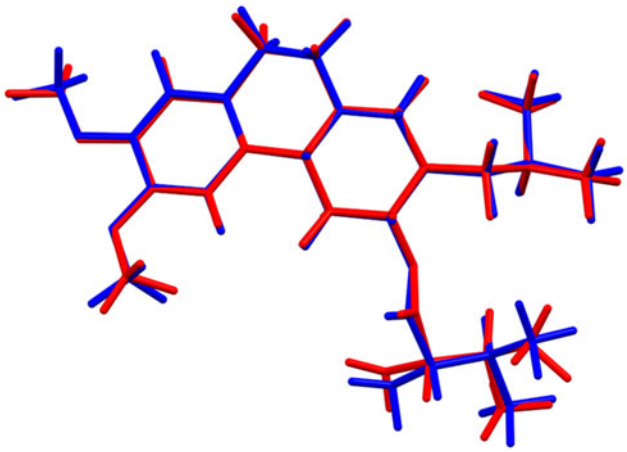

Figure 4. Comparison of the Rietveld-refined (red) and VASP-optimized (blue) structures of the valbenazine. The rms Cartesian displacement is 0.142 Å. Image generated using Mercury (Macrae et al., 2020).

Rietveld refinement (Figure 2) was carried out with GSAS-II (Toby and Von Dreele, 2013). Only the 1.7–22.0° portion of the pattern was included in the refinements (d_{min} = 1.205 Å). All non-H-bond distances and angles were subjected to restraints, based on a Mercury/Mogul Geometry Check (Bruno et al., 2004; Sykes et al., 2011). The Mogul average and standard deviation for each quantity were used as the restraint parameters. The phenyl ring was restrained to be planar. The hydrogen atoms were included in calculated positions, which were recalculated during the refinement using Materials Studio (Dassault, 2022) using the Adjust Hydrogen tool. The U_{iso} of the heavy atoms were grouped by chemical similarity. The U_{iso} for the H atoms was fixed at 1.3× the U_{iso} of the heavy atoms to which they are attached. The peak profiles were described using the generalized microstrain model (Stephens, 1999). The final Rietveld plot is shown in Figure 2. The largest features in the normalized error plot represent subtle shifts in peak positions and may represent change to the specimen during the measurement.

The crystal structure of valbenazine was optimized (fixed experimental unit cell) with density functional techniques using VASP (Kresse and Furthmüller, 1996) through the MedeA graphical interface (Materials Design, 2016). The calculation was carried out on 16 2.4 GHz processors (each with 4 Gb RAM) of a 64-processor HP Proliant DL580 Generation 7 Linux cluster at North Central College. The calculation used the GGA-PBE functional, a plane wave cutoff energy of 400.0 eV, and a *k*-point spacing of 0.5 $Å^{-1}$ leading to a 3 × 1 × 1 mesh, and took ∼9.5 days. Single-point density functional theory calculations (fixed experimental cell) and population analysis were carried out using CRYSTAL23 (Erba et al., 2023). The basis sets for the H, C, N, and O atoms in the calculation were those of Gatti et al. (1994). The calculations were run on a 3.5 GHz PC using 14 *k*-points and the B3LYP functional and took ∼3.6 h.

III. RESULTS AND DISCUSSION

The powder pattern of this study is similar enough to that reported by Langes and Reissmann (2018; Figure 3) to conclude that they represent the same material. The material

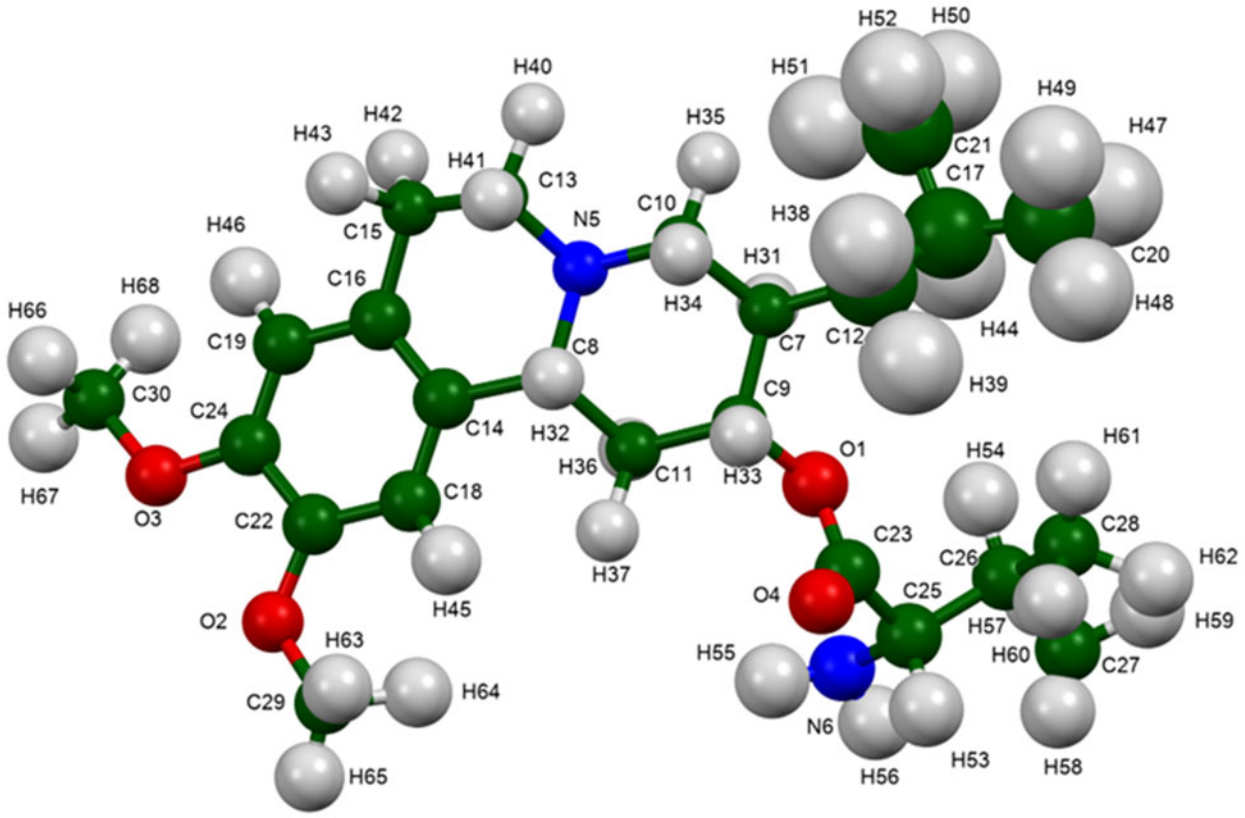

Figure 5. The asymmetric unit of valbenazine, with the atom numbering. The atoms are represented by 50% probability spheroids. Image generated using Mercury (Macrae et al., 2020).

https://doi.org/10.1017/S0885715624000198 Published online by Cambridge University Press

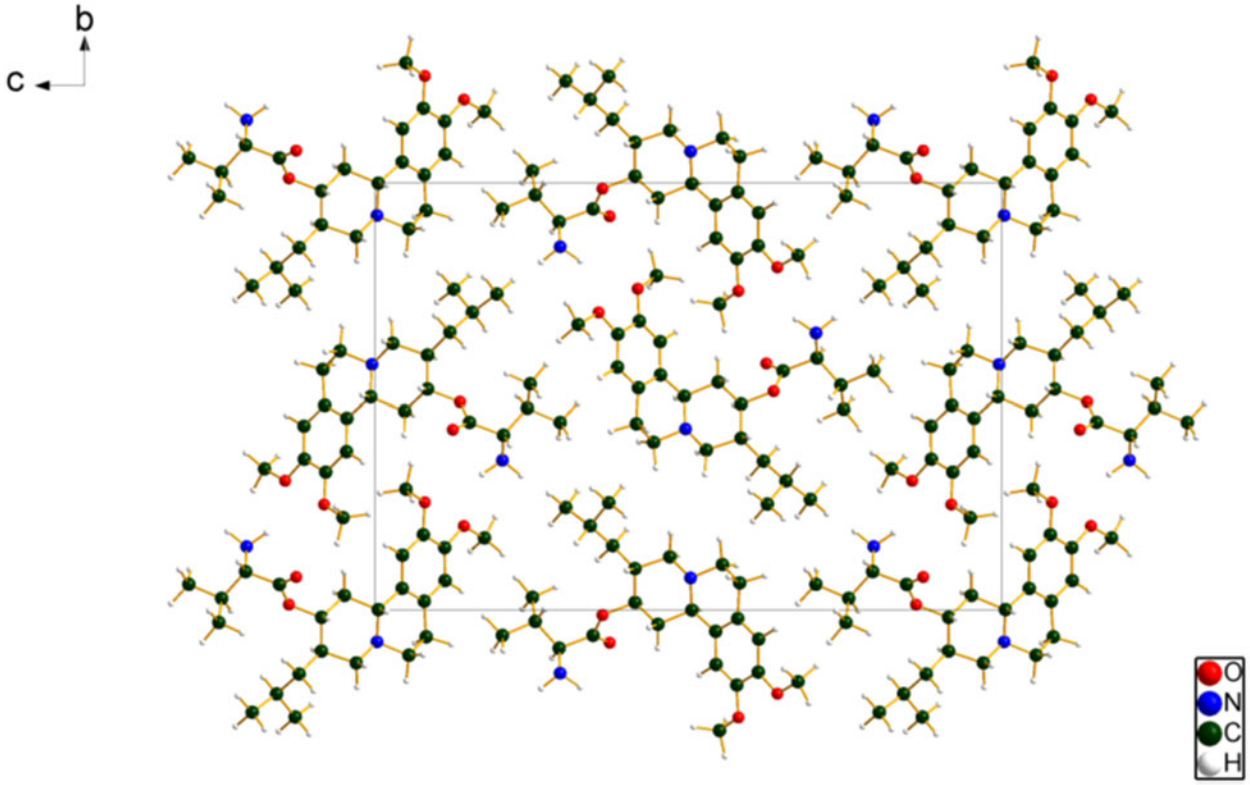

Figure 6. The crystal structure of valbenazine, viewed down the *a*-axis. Image generated using Diamond (Crystal Impact, 2022).

analyzed in this study is probably representative of that used in commerce. The root-mean-square Cartesian displacement of the non-H atoms in the Rietveld-refined and VASP-optimized molecules is 0.142 Å (Figure 4). The agreement is within the normal range for correct structures (van de Streek and Neumann, 2014). The asymmetric unit with the atom numbering is presented in Figure 5. The remainder of this discussion will emphasize the VASP-optimized structure.

All of the bond distances and bond angles fall within the normal ranges indicated by a Mercury Mogul Geometry check (Macrae et al., 2020). The torsion angles involving rotation about the C7–C12 and C23–C25 bonds are flagged as unusual, but they lie in the middle of broad distributions with few hits. Quantum chemical geometry optimization of the isolated molecule (DFT/B3LYP/6-31G*/water) using Spartan '20 (Wavefunction, 2022) indicated that the solid-state conformation is 3.1 kcal/mol higher in energy than a local minimum, which has a very similar conformation. The global minimum energy conformation is 8.9 kcal/mol lower in energy and has different orientations of the methoxy and peripheral groups. The difference shows that, while weak, the hydrogen bonds affect the observed conformation.

The crystal structure (Figure 6) consists of discrete molecules. The mean plane of the molecule is approximately (8,−2,15). There are no obvious strong intermolecular interactions. Analysis of the contributions to the total crystal energy of the structure using the Forcite module of Materials Studio (Dassault Systèmes, 2022) suggests that bond, angle, and torsion distortion terms contribute significantly to the intramolecular deformation energy, but that angle terms are the most important, as expected for a molecule containing a fused ring system. The intermolecular energy is dominated by electrostatic repulsions, with a significant contribution from van der Waals attractions.

There is only one classical hydrogen bond in the structure (Table I), from the amino group N6 to the ether oxygen atom O3. This hydrogen bond is weak, and its energy was calculated using the correlation of Wheatley and Kaduk (2019). Two intramolecular and one intermolecular C–H···O hydrogen bonds also contribute to the lattice energy.

The volume enclosed by the Hirshfeld surface of valbenazine (Figure 7, Hirshfeld, 1977; Spackman et al., 2021) is 603.16 Å^3, 98.64% of the unit cell volume. The packing density is thus fairly typical. The only significant close contacts

TABLE I. Hydrogen bonds (CRYSTAL23) in valbenazine

H-Bond	D–H, Å	H···A, Å	D···A, Å	D–H···A,◦	Overlap, *e*	*E*, kcal/mol
N6–H55···O3	1.026	2.382	3.225	138.7	0.017	3.0
C11–H36···O4	1.100	2.408	3.424	153.0	0.014	
C9–H33···O4	1.103	2.304[a]	2.710	99.3	0.013	
C26–H54···O1	1.102	2.473[a]	2.849	98.3	0.010	

[a]Intramolecular.

https://doi.org/10.1017/S0885715624000198 Published online by Cambridge University Press

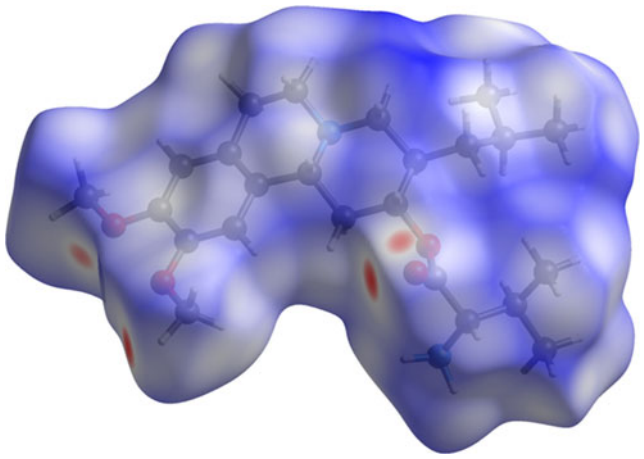

Figure 7. The Hirshfeld surface of valbenazine. Intermolecular contacts longer than the sums of the van der Waals radii are colored blue, and contacts shorter than the sums of the radii are colored red. Contacts equal to the sums of radii are white. Image generated using CrystalExplorer (Spackman et al., 2021).

(red in Figure 7) involve the hydrogen bonds. The volume/non-hydrogen atom is larger than normal, at 20.4 Å^3.

The Bravais–Friedel–Donnay–Harker (Bravais, 1866; Friedel, 1907; Donnay and Harker, 1937) morphology suggests that we might expect needlelike morphology for valbenazine, as expected for stacking of the molecules along the short <100> axis. No preferred orientation model was necessary, indicating that preferred orientation was not present in this rotated capillary specimen.

IV. DEPOSITED DATA

The powder pattern of valbenazine from this synchrotron data set has been submitted to ICDD for inclusion in the Powder Diffraction File. The Crystallographic Information Framework (CIF) files containing the results of the Rietveld refinement (including the raw data) and the DFT geometry optimization were deposited with the ICDD. The data can be requested at pdj@icdd.com.

ACKNOWLEDGEMENTS

Use of the Advanced Photon Source at Argonne National Laboratory was supported by the U. S. Department of Energy, Office of Science, Office of Basic Energy Sciences, under Contract No. DE-AC02-06CH11357. This work was partially supported by the International Centre for Diffraction Data. We thank Saul Lapidus for his assistance in the data collection.

CONFLICTS OF INTEREST

The authors have no conflicts of interest to declare.

REFERENCES

Altomare, A., C. Cuocci, C. Giacovazzo, A. Moliterni, R. Rizzi, N. Corriero, and A. Falcicchio. 2013. "EXPO2013: A Kit of Tools for Phasing Crystal Structures from Powder Data." *Journal of Applied Crystallography* 46: 1231–5.

Antao, S. M., I. Hassan, J. Wang, P. L. Lee, and B. H. Toby. 2008. "State-of-the-Art High-Resolution Powder X-ray Diffraction (HRPXRD) Illustrated with Rietveld Refinement of Quartz, Sodalite, Tremolite, and Meionite." *Canadian Mineralogist* 46: 1501–9.

Bravais, A. 1866. *Etudes Cristallographiques*. Paris, Gauthier Villars.

Bruno, I. J., J. C. Cole, M. Kessler, J. Luo, W. D. S. Motherwell, L. H. Purkis, B. R. Smith, R. Taylor, R. I. Cooper, S. E. Harris, and A. G. Orpen. 2004. "Retrieval of Crystallographically-Derived Molecular Geometry Information." *Journal of Chemical Information and Computer Sciences* 44: 2133–44.

Crystal Impact. 2022. *Diamond. V. 4.6.8*. Crystal Impact - Dr. H. Putz & Dr. K. Brandenburg. Windows.

Dassault Systèmes. 2022. *Materials Studio 2023*. San Diego, CA, BIOVIA.

Donnay, J. D. H., and D. Harker. 1937. "A New Law of Crystal Morphology Extending the Law of Bravais." *American Mineralogist* 22: 446–47.

Erba, A., J. K. Desmaris, S. Casassa, B. Civalleri, L. Donà, I. J. Bush, B. Searle, L. Maschio, L.-E. Daga, A. Cossard, C. Ribaldone, E. Ascrizzi, N. L. Marana, J.-P. Flament, and B. Kirtman. 2023. "CRYSTAL23: A Program for Computational Solid State Physics and Chemistry." *Journal of Chemical Theory and Computation*. 19, 6891–932. doi: 10.1021/acs.jctc.2c00958.

Favre-Nicolin, V., and R. Černý. 2002. "FOX, Free Objects for Crystallography: A Modular Approach to Ab Initio Structure Determination from Powder Diffraction." *Journal of Applied Crystallography* 35: 734–43.

Friedel, G. 1907. "Etudes sur la loi de Bravais." *Bulletin de la Société Française de Minéralogie* 30: 326–455.

Gates-Rector, S., and T. N. Blanton. 2019. "The Powder Diffraction File: A Quality Materials Characterization Database." *Powder Diffraction* 39: 352–60.

Gatti, C., V. R. Saunders, and C. Roetti. 1994. "Crystal-Field Effects on the Topological Properties of the Electron-Density in Molecular Crystals – The Case of Urea." *Journal of Chemical Physics* 101: 10686–96.

Groom, C. R., I. J. Bruno, M. P. Lightfoot, and S. C. Ward. 2016. "The Cambridge Structural Database." *Acta Crystallographica Section B: Structural Science, Crystal Engineering and Materials* 72: 171–9.

Hirshfeld, F. L. 1977. "Bonded-Atom Fragments for Describing Molecular Charge Densities." *Theoretica Chemica Acta* 44: 129–38.

Kaduk, J. A., C. E. Crowder, K. Zhong, T. G. Fawcett, and M. R. Suchomel. 2014. "Crystal Structure of Atomoxetine Hydrochloride (Strattera), $C_{17}H_{22}NOCl$." *Powder Diffraction* 29: 269–73.

Kim, S., J. Chen, T. Cheng, A. Gindulyte, J. He, S. He, Q. Li, B. A. Shoemaker, P. A. Thiessen, B. Yu, L. Zaslavsky, J. Zhang, and E. E. Bolton. 2023. "Pubchem 2023 Update." *Nucleic Acids Research* 51 (D1): D1373–80. doi:10.1093/nar/gkac956.

Kresse, G., and J. Furthmüller. 1996. "Efficiency of Ab-Initio Total Energy Calculations for Metals and Semiconductors Using a Plane-Wave Basis Set." *Computational Materials Science* 6: 15–50.

Langes, C., and S. Reissmann. 2018. "Crystalline Valbenazine Free Base." International Patent Application WO 2018/130345 A1.

Lee, P. L., D. Shu, M. Ramanathan, C. Preissner, J. Wang, M. A. Beno, R. B. Von Dreele, L. Ribaud, C. Kurtz, S. M. Antao, X. Jiao, and B. H. Toby. 2008. "A Twelve-Analyzer Detector System for High-Resolution Powder Diffraction." *Journal of Synchrotron Radiation* 15: 427–32.

Macrae, C. F., I. Sovago, S. J. Cottrell, P. T. A. Galek, P. McCabe, E. Pidcock, M. Platings, G. P. Shields, J. S. Stevens, M. Towler, and P. A. Wood. 2020. "*Mercury 4.0*: From Visualization to Design and Prediction." *Journal of Applied Crystallography* 53: 226–35.

Materials Design. 2016. *MedeA 2.20.4*. Angel Fire, NM, Materials Design Inc.

McGee, K., S. Zook, A. Carr, & T. Bonnaud. 2017. "Valbenazine Salts and Polymorphs Thereof." International Patent Application 2017/075340.

MDI. 2023. *JADE Pro version 9.0*. Livermore, CA, Materials Data.

O'Boyle, N. M., M. Banck, C. A. James, C. Morley, T. Vandermeersch, and G. R. Hutchison. 2011. "Open Babel: An Open Chemical Toolbox." *Journal of Chemical Informatics* 3: 33. doi:10.1186/1758-2946-3-33.

Silk Scientific. 2013. *UN-SCAN-IT 7.0*. Orem, UT, Silk Scientific Corporation.

Spackman, P. R., M. J. Turner, J. J. McKinnon, S. K. Wolff, D. J. Grimwood, D. Jayatilaka, and M. A. Spackman. 2021. "Crystalexplorer: A Program for Hirshfeld Surface Analysis, Visualization and Quantitative Analysis of Molecular Crystals." *Journal of Applied Crystallography* 54: 1006–11. doi:10.1107/S1600576721002910.

Stephens, P. W. 1999. "Phenomenological Model of Anisotropic Peak Broadening in Powder Diffraction." *Journal of Applied Crystallography* 32: 281–9.

Sykes, R. A., P. McCabe, F. H. Allen, G. M. Battle, I. J. Bruno, and P. A. Wood. 2011. "New Software for Statistical Analysis of Cambridge Structural Database Data." *Journal of Applied Crystallography* 44: 882–6.

Toby, B. H., and R. B. Von Dreele. 2013. "GSAS II: The Genesis of a Modern Open Source All Purpose Crystallography Software Package." *Journal of Applied Crystallography* 46: 544–9.

van de Streek, J., and M. A. Neumann. 2014. "Validation of Molecular Crystal Structures from Powder Diffraction Data with Dispersion-Corrected Density Functional Theory (DFT-D)." *Acta Crystallographica Section B: Structural Science, Crystal Engineering and Materials* 70: 1020–32.

Wang, J., B. H. Toby, P. L. Lee, L. Ribaud, S. M. Antao, C. Kurtz, M. Ramanathan, R. B. Von Dreele, and M. A. Beno. 2008. "A Dedicated Powder Diffraction Beamline at the Advanced Photon Source: Commissioning and Early Operational Results." *Review of Scientific Instruments* 79: 085105.

Wavefunction, Inc. 2022. *Spartan '20. V. 1.1.4*. Irvine, CA, Wavefunction Inc.

Wheatley, A. M., and J. A. Kaduk. 2019. "Crystal Structures of Ammonium Citrates." *Powder Diffraction* 34: 35–43.

https://doi.org/10.1017/S0885715624000198 Published online by Cambridge University Press